

Vim-F: Visual State Space Model Benefiting from Learning in the Frequency Domain

Juntao Zhang¹, Shaogeng Liu¹, Kun Bian^{2,1}, You Zhou^{2,1}, Pei Zhang³, Wenbo An¹, Jun Zhou¹ and Kun Shao¹

¹AMS, Beijing, China

²School of Electronic Engineering, Xidian University

³Coolanyp L.L.C., Wuxi, China

Abstract—In recent years, State Space Models (SSMs) with efficient hardware-aware designs, known as the Mamba deep learning models, have made significant progress in modeling long sequences. Compared to traditional convolutional neural networks (CNNs) and Vision Transformers (ViTs), the performance of Vision Mamba (ViM) methods is not yet fully competitive. To enable SSMs to process image data, ViMs typically flatten 2D images into 1D sequences, inevitably ignoring some 2D local dependencies, thereby weakening the model’s ability to interpret spatial relationships from a global perspective. We believe that the introduction of frequency domain information can enable ViM to achieve a better global receptive field during the scanning process. We propose a novel model called Vim-F, which employs pure Mamba encoders and scans in both the frequency and spatial domains. Moreover, we question the necessity of position embedding in ViM and remove it accordingly in Vim-F, which helps to fully utilize the efficient long-sequence modeling capability of ViM. Finally, we redesign a patch embedding for Vim-F, leveraging a convolutional stem to capture more local correlations, further improving the performance of Vim-F. Code is available at: <https://github.com/yws-wxs/Vim-F>.

Index Terms—Vision Mamba, State Space Model, Fast Fourier Transform, Scanning strategy

I. INTRODUCTION

Visual representation learning stands as a pivotal research topic within the realm of computer vision. In the early era of deep learning, Convolutional Neural Networks (CNNs) occupied a dominant position. CNNs have several built-in inductive biases that make them well-suited to a wide variety of computer vision applications. In addition, CNNs are inherently efficient because when used in a sliding-window manner, the computations are shared. Inspired by the significant success of the Transformer architecture in the field of Natural Language Processing (NLP), researchers have recently applied Transformer to computer vision tasks. Except for the initial “patch embedding” module, which splits an image into a sequence of patches, Vision Transformers (ViTs) do not introduce image-specific inductive biases and follow the original NLP Transformers design concept as much as possible. Compared to CNNs, ViTs typically exhibit superior performance, which can be attributed to the global receptive field and dynamic weights facilitated by the attention mechanism. However, the attention mechanism requires quadratic complexity in terms of image sizes, resulting in significant computational cost when addressing downstream dense prediction tasks, such as object detection and instance segmentation.

Derived from the classic Kalman filter model, modern State Space Models (SSMs) excel at capturing long-range dependencies and reap the benefits of parallel training. The Visual Mamba Models (ViMs) [1]–[4], which are inspired by recently proposed SSMs [5], [6], utilize the Selective Scan Space State Sequential Model (S6) to compress previously scanned information into hidden states, effectively reducing quadratic complexity to linear. Most of these studies integrate the original SSM structure of Mamba into their basic models, thereby necessitating the conversion of 2D images into 1D sequences for SSM-based processing. However, due to the non-causal nature of visual data, flattening spatial data into one-dimensional tokens destroys local two-dimensional dependencies, impairing the model’s capacity to accurately interpret spatial relationships. Vim [1] addresses this issue by scanning in bidirectional horizontal directions, while VMamba [2] adds vertical scanning, enabling each element in the feature map to integrate information from other locations in different directions. Subsequent works, such as LocalMamba [3] and EfficientVMamba [4], have designed a series of novel scanning strategies in the spatial domain, aimed at capturing local dependencies while maintaining a global view. We believe that these strategies do not significantly enhance the model’s ability to obtain a better global receptive field. These efforts have prompted us to focus on the value of scanning in the frequency domain. We know that the use of 2D Discrete Fourier transform (DFT) to convert feature maps into spectrograms does not alter their shapes. The value $P(x, y)$ at any point (x, y) in the spectrogram depends on the entire original feature map. Therefore, scanning in the frequency domain ensures that the model always has a good global receptive field. On the other hand, without considering spectral shifts, the high-frequency components are located in the corners of the spectrogram, whereas the low-frequency components are centered. Scanning across the spectrogram typically alternates between accessing low and high frequencies, which may facilitate balanced modeling. Therefore, we adopt the most direct solution, which is to add the amplitude spectrum of the feature map to the original feature map, allowing the visual Mamba encoder to learn the fused semantic information. Using the Fast Fourier Transform (FFT) algorithm to calculate the amplitude spectrum not only introduces no trainable parameters but also has minimal impact on performance. To clearly demonstrate the effectiveness and ease of use of our work,

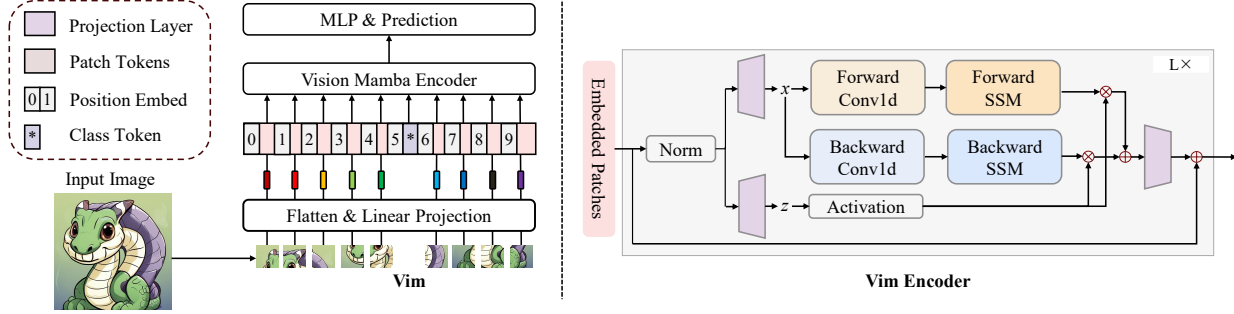


Fig. 1. The overview of the Vim model.

we chose Vim as the base model, which to our knowledge is the first pure-SSM-based visual model. Based on the open-source code provided by the authors, our method, called Vim-F, can be easily implemented by adding a few lines of code. Secondly, we improve the patch embedding to capture more local dependencies. Many successful lightweight transformer models, such as EfficientFormer [7] and MobileViT [8], start their networks with a convolutional stem as patch embedding. This is attributed to the inherent spatial inductive bias of CNN, which is beneficial for capturing local information. In addition, CNNs are less sensitive to data augmentation, and the training process of a hybrid architecture is more stable. Inspired by these works, we design a patch embedding for Vim-F. Specifically, we use multiple convolutional layers for downsampling and then flatten the feature maps. Finally, we argue that the Mamba model is essentially still a recurrent neural network (RNN). Therefore, Vim lacks the rationale for using positional embeddings, and thus our Vim-F does not employ positional embeddings. Additionally, we reduce the model's sensitivity to the order of input sequences by alternately stacking linear attention blocks and Vim-F blocks, while maintaining overall linear complexity. We refer to this hybrid architecture as Vim-F(H). We outline our contributions below:

- Based on Vim [1], we propose Vim-F, which enables SSM to scan both in the spatial and frequency domains, ensuring that SSM always has a global view during the scanning process, thereby enhancing the model's ability to interpret spatial relationships. To the best of our knowledge, our work is the first to propose scanning in the frequency domain.
- We design a novel patch embedding module that utilizes a mixture of overlapping and non-overlapping convolutions with small kernel sizes to downsample the feature map and then flatten it. Additionally, we question the necessity of position embedding in Vim, thus Vim-F does not utilize position embedding.
- The experimental results demonstrate that the simple Vim variant, Vim-F, achieves better performance while maintaining similar computational costs and parameters. Additionally, introducing linear attention to reduce Vim-F's sensitivity to the order of input sequences can further

enhance the model's performance.

II. RELATED WORKS

A. State Space Models

In mathematics, State Space Models (SSMs) are usually expressed as linear ordinary differential equations (ODEs). These models transform input D -dimensional sequence $x(t) \in \mathbb{R}^{L \times D}$ into output sequence $y(t) \in \mathbb{R}^{L \times D}$ by utilizing a learnable latent state $h(t) \in \mathbb{R}^{L \times N}$ that is not directly observable. The mapping process could be denoted as:

$$\begin{aligned} h'(t) &= \mathbf{A}h(t) + \mathbf{B}x(t), \\ y(t) &= \mathbf{C}h(t), \end{aligned} \quad (1)$$

where $\mathbf{A} \in \mathbb{R}^{N \times N}$, $\mathbf{B} \in \mathbb{R}^{D \times N}$ and $\mathbf{C} \in \mathbb{R}^{N \times D}$.

B. Overview of Vim

As mentioned earlier, the effectiveness of our work is demonstrated through the improvement of Vim. Therefore, we provide a brief introduction to the overall architecture of Vim. As shown in Fig. 1, Vim first reshapes the 2D image $\mathbf{X} \in \mathbb{R}^{h \times w \times c}$ into a sequence of flattened 2D patches $\mathbf{X}_p \in \mathbb{R}^{n \times (p^2 \cdot c)}$, where c is the number of channels, (h, w) is the resolution of the original image, and (p, p) is the resolution of each image patch. The effective sequence length for Vim is therefore $n = hw/p^2$. Then, Vim linearly projects \mathbf{X}_p into vectors of size d and adds them to the position embeddings $\mathbf{E}_{pos} \in \mathbb{R}^{(n+1) \times d}$, as follows:

$$\mathbf{T}_0 = [\mathbf{X}_{cls}; \mathbf{X}_p^1 \mathbf{W}; \mathbf{X}_p^2 \mathbf{W}; \dots; \mathbf{X}_p^i \mathbf{W}; \dots; \mathbf{X}_p^d \mathbf{W}] + \mathbf{E}_{pos}, \quad (2)$$

where \mathbf{X}_p^i is the i -th patch of \mathbf{X} , $\mathbf{W} \in \mathbb{R}^{(p^2 \cdot c) \times d}$ is the learnable projection matrix. Vim uses class token to represent the whole patch sequence, which is denoted as \mathbf{X}_{cls} . Vim then sends the token sequence (\mathbf{T}_{l-1}) to the l -th layer of the Vim encoder, and gets the output \mathbf{T}_l . Finally, Vim normalizes the output class token \mathbf{T}_L^0 and feeds it to the multi-layer perceptron (MLP) head to get the final prediction \hat{p} , as follows:

$$\begin{aligned} \mathbf{T}_l &= \mathbf{Vim}(\mathbf{T}_{l-1}) + \mathbf{T}_{l-1}, \\ f &= \mathbf{Norm}(\mathbf{T}_L^0), \\ \hat{p} &= \mathbf{MLP}(f), \end{aligned} \quad (3)$$

where **Vim** is the proposed vision mamba block, L is the number of blocks, and **Norm** is the normalization layer.

III. RETHINKING THE SCANNING STRATEGY OF ViMs

The non-causal nature of two-dimensional spatial patterns in images is inherently inconsistent with the causal processing framework of SSM. Therefore, it is meaningful to explore methods for serializing images. However, the majority of existing work on scanning strategies is typically based on a rather idealized assumption that introducing more or more complex inductive biases regarding the order of one-dimensional sequences can potentially enhance Mamba's ability to understand local image correlations. Theoretically, regardless of the order, reducing the distance between adjacent tokens in one direction in two-dimensional space inevitably increases the distance between adjacent tokens in another direction, thus these strategies are essentially equivalent. Additionally, in the absence of global information serving as a "frame of reference," these sorting methods are essentially disconnected, making it inherently difficult for Mamba to gain additional spatial relationship information by scanning multiple sequences. In practice, works involving scanning strategy research, including Vim [1], VMamba [2], LocalMamba [3], EfficientVMamba [4], and PlainMamba [9], lack clear comparative experiments to verify the necessity and effectiveness of their scanning strategies. Zhu et al. [10] conduct a comprehensive experimental investigation on the impact of mainstream scanning directions and their combinations on semantic segmentation of remotely sensed images. Through extensive experiments on the LoveDA, ISPRS Potsdam, and ISPRS Vaihingen datasets, they demonstrate that no single scanning strategy outperforms others, regardless of their complexity or the number of scanning directions involved. In summary, an effective scanning strategy needs to maintain a global receptive field throughout the scanning process and demonstrate its effectiveness through analysis and comparative experiments.

IV. METHODOLOGY

In this section, we first elaborate on the significance and benefits of frequency-domain scanning. Subsequently, we present the specific details of patch embedding in Vim-F. Finally, we discuss the composition of the Vim-F and the Vim-F(H) block.

A. 2D Scanning in the Frequency Domain

The flattening method used in Vim [1] disrupts these local dependencies and significantly increases the distance between vertically adjacent tokens. We address this limitation by introducing frequency-domain scanning. Specifically, we first perform a Fourier transform on the feature map to obtain:

$$F(u, v) = \sum_{x=0}^{M-1} \sum_{y=0}^{N-1} f(x, y) e^{-j2\pi(\frac{ux}{H} + \frac{vy}{W})}, \quad (4)$$

where j represents the imaginary unit, H and W represent the height and width of the feature map, respectively. $f(x, y) \in \mathbb{R}^{H \times W}$ represents the corresponding value at the

coordinate (x, y) in the feature map, and $F(u, v)$ represents the corresponding value at the coordinate (u, v) in the frequency domain. $|F(u, v)| \in \mathbb{R}^{H \times W}$ represents the modulus of $F(u, v)$, which is also known as the amplitude spectrum. Fourier transform has translation invariance. In other words, if a function is translated in the spatial domain, its Fourier transform remains the same as the original function. This property is quite meaningful for addressing the issue of increasing distances between vertically adjacent tokens, as shown in Fig. 2. The amplitude spectra of figures (a) and (b) are identical, so scanning in the frequency domain helps reduce the inductive bias introduced by the scanning strategy. Therefore, frequency domain scanning does not require fancy strategies, and it can be consistent with Vim's original spatial domain scanning strategy.

B. Patch Embedding

In Vim and ViTs, the patching strategy typically involves using large convolutional kernels (such as kernel sizes of 14 or 16) with non-overlapping convolutions. However, VMamba and Swin Transformer utilize non-overlapping convolutions with a kernel size of 4, indicating that current ViMs haven't undergone much targeted design in terms of patching. We believe that non-overlapping convolutions have fewer inductive biases, and the self-attention mechanism of the Transformer architecture excels at modeling relationships between patches. Therefore, adopting non-overlapping convolutions can benefit the performance of Transformers. On the contrary, the additional correlation between patches introduced by overlapping convolutions can be advantageous for the scanning mechanism of ViMs.

Based on the above analysis, we can try to explain why Vim uses the position embedding. The bidirectional horizontal scanning strategy employed by Vim makes adjacent tokens in horizontal and vertical directions far apart in the sequence. In addition, the lack of data correlation between tokens makes it difficult for the model to understand the spatial relationship in the vertical direction. The introduction of the trainable position embedding can explicitly provide the model with the absolute position of each token in the plane space, thus alleviating the above problems. In contrast, it is simpler and more flexible to remove the position embedding and establish spatial correlation through overlapping convolutions, enabling the model to learn spatial positional relationships.

Specifically, we first utilize a 7×7 convolutional layer with a stride of 4 to model the local correlation of the input image. Then, we downsample the feature map twice through two downsampling blocks. Each downsampling block consists of a 2×2 convolutional layer with a stride of 2 and a 1×1 convolutional layer. The details of the adaptation with the two base models [1] (Vim-Ti and Vim-S) are shown in Table I.

The patch embedding in Vim can be implemented through a 16×16 convolutional layer with a stride of 16. The convolutional stem for patch embedding in Vim-F comprises more convolutional layers, but the additional computational cost is negligible due to the use of smaller convolutional kernels.

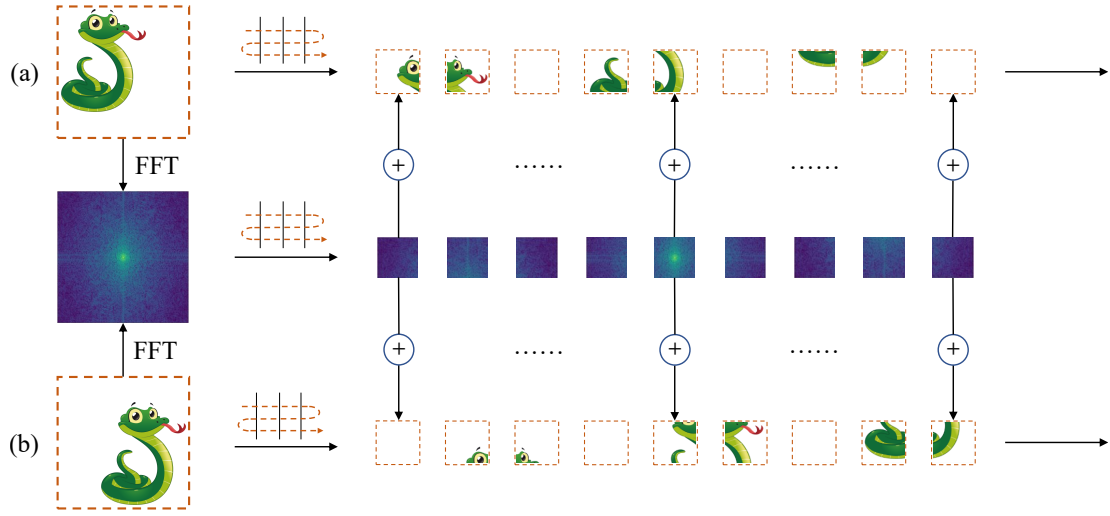


Fig. 2. Illustrating the scanning strategy of Vim-F through an example of forward scanning in both the frequency and spatial domains. Due to the translation invariance of the Fourier transform, the Fourier transforms of figures (a) and (b) are identical.

TABLE I
CONVOLUTIONAL STEM FOR PATCH EMBEDDING.

	Output size	Vim-Ti	Vim-S
Block1	56×56	$7 \times 7, 48, \text{stride } 4$ padding 3	$7 \times 7, 48, \text{stride } 4$ padding 3
Block2	28×28	$\begin{bmatrix} 2 \times 2, 96, \text{stride } 2 \\ 1 \times 1, 96 \end{bmatrix}$	$\begin{bmatrix} 2 \times 2, 192, \text{stride } 2 \\ 1 \times 1, 192 \end{bmatrix}$
Block3	14×14	$\begin{bmatrix} 2 \times 2, 192, \text{stride } 2 \\ 1 \times 1, 192 \end{bmatrix}$	$\begin{bmatrix} 2 \times 2, 384, \text{stride } 2 \\ 1 \times 1, 384 \end{bmatrix}$

Considering Vim-Ti as the baseline model, the computational load measured in GFLOPs only increases by 0.035.

C. Vim-F Block

As mentioned earlier, the Vim-F block is an improvement over the Vim block, as shown in Fig. 3. Specifically, a 2D FFT is performed on the input to obtain the spectrogram. Then, the spectrogram is added to the original input, with the intensity of the frequency and spatial domain information being adjusted by two trainable parameters, α and β , respectively. After the linear layer mixes the hidden dimensions of the feature map, the cross-domain information is sent to the Vim block for processing.

Vim-F requires a 2D discrete Fourier transform (DFT) to be performed on the feature map before scanning, thus introducing additional computation. The Cooley-Tukey FFT algorithm decomposes a DFT of a sequence with length N into two DFTs of sub-sequences with length $N/2$, significantly reducing the computational complexity. During the execution of the algorithm, the data is divided into two parts based on whether they are odd or even, and the DFTs of each part are computed separately before merging the results. For a 2D-DFT

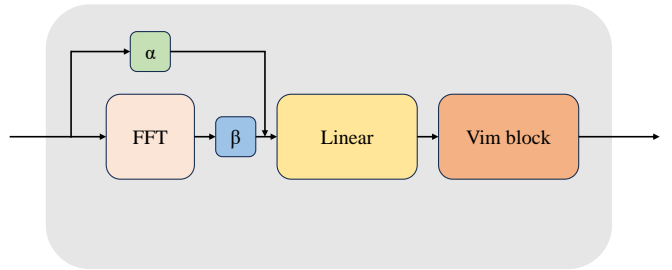


Fig. 3. Vim-F block

with dimensions (L, D) , its complexity is $\Omega(L \cdot D \cdot \log L \cdot \log D)$. The feedforward network is implemented by a linear layer, with a complexity of $\Omega(L \cdot D^2)$. Therefore, compared to the Vim block, the additional overhead of the Vim-F block is approximately linearly related to the sequence length L .

D. Vim-F(H) Block

Observing Eq. (1), it is evident that since all elements of matrix A are strictly confined within the range of 0 to 1 [5], the early information stored in the hidden state h will continuously decay. This leads to Mamba being sensitive to the order of the input sequence. We propose that by weighting the input sequence with attention mechanisms before processing with Mamba, this strong local bias can be mitigated, thereby enhancing Mamba's capability to handle long sequences. We integrate the Vim-F block with the linear attention [11] to maintain approximately linear complexity, which we term Vim-F(H), and its structure is depicted in Fig. 4.

V. EXPERIMENTS

This section presents our experimental results, starting with the ImageNet classification task and then transferring the trained model to various downstream tasks, including object detection and instance segmentation. The specific architectures

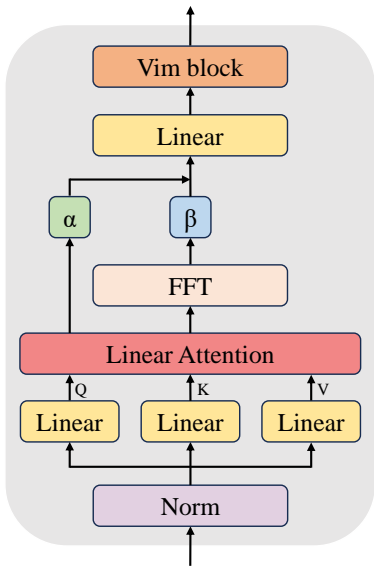


Fig. 4. Vim-F(H) block

TABLE II
COMPARISON OF DIFFERENT BACKBONES ON IMAGENET-1K
CLASSIFICATION.

Method	Params (M)	FLOPs (G)	Top-1 (%)
PVTv2-B0 [12]	3	0.6	70.5
DeiT-Ti [13]	6	1.3	74.4
MobileViT-XS [14]	2	1.0	74.8
LVT [15]	6	0.9	74.8
Vim-Ti [1]	7	1.5	76.1
LocalVim-T [3]	8	1.5	76.5
Vim-Ti-F (ours)	8	1.8	76.7
PlainMamba-L1 [9]	7	3.0	77.9
RegNetY-1.6G [16]	11	1.6	78.0
Vim-Ti-F(H) (ours)	9	2.1	78.2
MobileViT-S [14]	6	2.0	78.4
EfficientVMamba-S [4]	11	1.3	78.7
DeiT-S [13]	22	4.6	79.8
RegNetY-4G [16]	21	4.0	80.0
Vim-S [1]	26	5.1	80.5
Vim-S-F (ours)	28	6.1	80.9
LocalVim-S [3]	28	4.8	81.0
Swin-T [17]	29	4.5	81.3
Vim-S-F(H) (ours)	37	6.8	81.6
EfficientVMamba-B [4]	33	4.0	81.8
VMamba-T [2]	22	5.6	82.2

of Vim-F and Vim-F(H) are as follows: We replaced only the first 6 Vim blocks (25% of the total number of blocks) with either Vim-F or Vim-F(H) blocks to balance performance and efficiency while maintaining approximately the same number of parameters. The number of linear attention heads in Vim-F(H) is set to 24.

A. Image Classification

Settings. We train the models on ImageNet-1K and evaluate the performance on ImageNet-1K validation set. For fair comparisons, our training settings mainly follow Vim. Due to hardware limitations, our experiments are performed on 3 A6000 GPUs. Therefore, we adjust the total batch size and the initial learning rate to 384 and 3.75×10^{-4} respectively according to the linear scaling rule [18].

Results. We selected advanced CNNs, ViTs, and ViMs with comparable parameters and computational costs in recent years to compare with our method, and the results are shown in Table II. Vim-F outperforms the original Vim in terms of performance, and Vim-F(H) further enhances Vim-F's performance by introducing linear attention. It is worth noting that SOTA ViMs such as VMamba [2], PlainMamba [9], and EfficientVMamba [4] all adopt more complex CNN-Mamba hybrid encoding architectures, and their network structures are similar to advanced convolutional networks like ConvNeXt [19]. Since these works have not conducted the necessary comparative experiments to address this issue, it is reasonable to suspect that the excellent performance of these ViMs may primarily stem from the use of depthwise separable convolutions. However, Vim-F still uses a pure SSM encoder to model visual information. LocalVim [3] is one of the representative works that improve the scanning strategy for Vim. LocalVim has designed 8 scanning strategies and employs neural architecture search to determine the scanning strategy used by each of the 4 scanning branches in every LocalVim block. Additionally, it utilizes a complex spatial and channel attention module (SCAttn) to weight the channels and tokens in each branch feature. Moreover, the total number of blocks in LocalVim has not followed Vim's 24 but has been reduced to 20. In comparison, our works achieve a better balance between performance, efficiency, and model complexity.

B. Object Detection and Instance Segmentation

Settings. We use Mask-RCNN as the detector to evaluate the performance of the proposed Vim-F for object detection and instance segmentation on the MSCOCO 2017 dataset. Since the backbone of Vim-F is non-hierarchical, following ViTDet [20], we only used the last feature map from the backbone and generated multi-scale feature maps through a set of convolutions or deconvolutions to adapt to the detector. The remaining settings were consistent with Swin [17]. Specifically, we employ the AdamW optimizer and fine-tune the pre-trained classification models (on ImageNet-1K) for both 12 epochs ($1 \times$ schedule). The learning rate is initialized at 1×10^{-4} and is reduced by a factor of $10 \times$ at the 9th and 11th epochs.

Results. We summarize the comparison results of Vim-F and Vim-F(H) with other backbones in Table III. It can be seen that our Vim-F consistently outperforms Vim. Similar to the results in classification tasks, Vim-F(H) exhibits better performance than Vim-F and is competitive with advanced ViT architectures.

TABLE III
OBJECT DETECTION AND INSTANCE SEGMENTATION RESULTS ON COCO.

Backbone	Params	FLOPs	AP ^b	AP ₅₀ ^b	AP ₇₅ ^b	AP ^m	AP ₅₀ ^m	AP ₇₅ ^m
ResNet-18	31M	207G	34.0	54.0	36.7	31.2	51.0	32.7
Vim-Ti	27M	189G	36.6	59.4	39.2	34.9	56.7	37.3
PVT-T	33M	208G	36.7	59.2	39.3	35.1	56.7	37.3
Vim-F-Ti (ours)	28M	189G	37.7	60.8	40.9	35.7	57.8	38.0
ResNet-50	44M	260G	38.0	58.8	41.4	34.7	55.7	37.2
Vim-F(H)-Ti (ours)	28M	189G	38.2	61.8	41.7	35.9	58.6	38.0
EfficientVMamba-S	31M	197G	39.3	61.8	42.6	36.7	58.9	39.2
ResNet-101	63M	336G	40.0	60.5	44.0	36.1	57.5	38.6
Vim-S	44M	272G	40.9	63.9	45.1	37.9	60.8	40.7
Vim-F-S (ours)	47M	273G	41.6	64.1	45.5	38.4	60.9	41.3
Swin-T	48M	267G	42.7	65.2	46.8	39.3	62.2	42.2
Vim-F(H)-S (ours)	57M	275G	42.9	65.4	47.1	39.2	62.1	42.1
Swin-S	69M	354G	44.8	66.6	48.9	40.9	63.2	44.2

VI. CONCLUSION

One of the main challenges currently faced by ViMs is the destruction of local two-dimensional dependency relationships when spatial data is flattened into one-dimensional tokens due to the non-causal nature of visual data. Consequently, scanning one-dimensional tokens with specific rules can limit the model’s ability to accurately interpret spatial relationships. We observe that scanning in the frequency domain, leveraging the translation invariance and global nature of Fourier transforms, can reduce the inductive bias of scanning strategies while ensuring that the model always maintains a good global receptive field. We adapt a simple approach of adding the spectrogram with the original feature map, allowing the model to scan simultaneously in both the frequency and spatial domains, thereby establishing a unified representation of visual information across both domains. Furthermore, we employ two trainable parameters to dynamically adjust the information intensity in the frequency and spatial domains, aiming to reduce semantic gaps. We also introduce additional local correlations during patch embedding by using overlapping convolutions. Vim-F(H) enhances the performance of Vim-F by introducing linear attention, which mitigates the sequence order sensitivity of the Mamba encoder. Extensive experiments demonstrate that our work effectively improves the performance of Vim, with Vim-F and Vim-F(H) achieving competitive results.

REFERENCES

- [1] Lianghui Zhu, Bencheng Liao, Qian Zhang, Xinlong Wang, Wenyu Liu, and Xinggang Wang, “Vision mamba: Efficient visual representation learning with bidirectional state space model,” *Preprint arXiv:2401.09417*, 2024.
- [2] Yue Liu, Yunjie Tian, Yuzhong Zhao, Hongtian Yu, Lingxi Xie, Yaowei Wang, Qixiang Ye, and Yunfan Liu, “Vmamba: Visual state space model,” *Preprint arXiv:2401.10166*, 2024.
- [3] Tao Huang, Xiaohuan Pei, Shan You, Fei Wang, Chen Qian, and Chang Xu, “Localmamba: Visual state space model with windowed selective scan,” *Preprint arXiv:2403.09338*, 2024.
- [4] Xiaohuan Pei, Tao Huang, and Chang Xu, “Efficientvmamba: Atrous selective scan for light weight visual mamba,” *Preprint arxiv:2403.09977*, 2024.
- [5] Albert Gu and Tri Dao, “Mamba: Linear-time sequence modeling with selective state spaces,” *Preprint arxiv:2312.00752*, 2023.
- [6] Harsh Mehta, Ankit Gupta, Ashok Cutkosky, and Behnam Neyshabur, “Long range language modeling via gated state spaces,” in *The Eleventh International Conference on Learning Representations (ICLR)*, 2023.
- [7] Yanyu Li, Geng Yuan, Yang Wen, Ju Hu, Georgios Evangelidis, Sergey Tulyakov, Yanzhi Wang, and Jian Ren, “Efficientformer: Vision transformers at mobilenet speed,” in *Annual Conference on Neural Information Processing Systems (NeurIPS)*, 2022.
- [8] Sachin Mehta and Mohammad Rastegari, “Mobilevit: Light-weight, general-purpose, and mobile-friendly vision transformer,” in *The Tenth International Conference on Learning Representations (ICLR)*, 2022.
- [9] Chenhongyi Yang, Zehui Chen, Miguel Espinosa, Linus Ericsson, Zhenyu Wang, Jiaming Liu, and Elliot J. Crowley, “Plainmamba: Improving non-hierarchical mamba in visual recognition,” in *35th British Machine Vision Conference 2024, BMVC 2024*.
- [10] Qinfeng Zhu, Yuan Fang, Yuanzhi Cai, Cheng Chen, and Lei Fan, “Rethinking scanning strategies with vision mamba in semantic segmentation of remote sensing imagery: An experimental study,” *arXiv*, vol. abs/2405.08493, 2024.
- [11] Angelos Katharopoulos, Apoorv Vyas, Nikolaos Pappas, and François Fleuret, “Transformers are rnns: Fast autoregressive transformers with linear attention,” in *Proceedings of the 37th International Conference on Machine Learning, ICML 2020*, vol. 119 of *Proceedings of Machine Learning Research*, pp. 5156–5165.
- [12] Wenhai Wang, Enze Xie, Xiang Li, Deng-Ping Fan, Kaitao Song, Ding Liang, Tong Lu, Ping Luo, and Ling Shao, “Pvt v2: Improved baselines with pyramid vision transformer,” *Computational Visual Media*, vol. 8, no. 3, pp. 415–424, 2022.
- [13] Hugo Touvron, Matthieu Cord, Matthijs Douze, Francisco Massa, Alexandre Sablayrolles, and Hervé Jégou, “Training data-efficient image transformers & distillation through attention,” in *International conference on machine learning (ICML)*, 2021, pp. 10347–10357.
- [14] Sachin Mehta and Mohammad Rastegari, “Mobilevit: light-weight, general-purpose, and mobile-friendly vision transformer,” *Preprint arXiv:2110.02178*, 2021.
- [15] Chenglin Yang, Yilin Wang, Jianming Zhang, He Zhang, Zijun Wei, Zhe Lin, and Alan Yuille, “Lite vision transformer with enhanced self-attention,” in *Proceedings of the IEEE Conference on Computer Vision and Pattern Recognition (CVPR)*, 2022, pp. 11998–12008.
- [16] Ilija Radosavovic, Raj Prateek Kosaraju, Ross Girshick, Kaiming He, and Piotr Dollár, “Designing network design spaces,” in *Proceedings of the IEEE conference on computer vision and pattern recognition (CVPR)*, 2020, pp. 10428–10436.
- [17] Ze Liu, Yutong Lin, Yue Cao, Han Hu, Yixuan Wei, Zheng Zhang, Stephen Lin, and Baining Guo, “Swin transformer: Hierarchical vision transformer using shifted windows,” in *2021 IEEE/CVF International Conference on Computer Vision (ICCV)*, 2021, pp. 9992–10002.
- [18] Priya Goyal, Piotr Dollár, Ross B. Girshick, Pieter Noordhuis, Lukasz Wesołowski, Aapo Kyrola, Andrew Tulloch, Yangqing Jia, and Kaiming

He, “Accurate, large minibatch SGD: training imagenet in 1 hour,” *Preprint arXiv:2111.11429*, 2017.

[19] Zhuang Liu, Hanzi Mao, Chao-Yuan Wu, Christoph Feichtenhofer, Trevor Darrell, and Saining Xie, “A convnet for the 2020s,” in *IEEE/CVF Conference on Computer Vision and Pattern Recognition, CVPR 2022*, pp. 11966–11976.

[20] Yanghao Li, Saining Xie, Xinlei Chen, Piotr Dollár, Kaiming He, and Ross B. Girshick, “Benchmarking detection transfer learning with vision transformers,” *Preprint arXiv:2111.11429*, 2021.